ACS chemical biology

Articles

pubs.acs.org/acschemicalbiology

A Short DNA Aptamer That Recognizes TNFα and Blocks Its Activity *in Vitro*

Erik W. Orava,[†,§] Nick Jarvik,[‖] Yuen Lai Shek,[†] Sachdev S. Sidhu,[‖] and Jean Gariépy*[,†,‡,§]

[†]Department of Pharmaceutical Sciences, Leslie Dan Faculty of Pharmacy, University of Toronto, 144 College Street, Toronto, Ontario M5S 3M2, Canada

[‡]Department of Medical Biophysics, University of Toronto, Toronto, Ontario M5G 2M9, Canada

[§]Physical Sciences, Sunnybrook Research Institute, 2075 Bayview Avenue, Toronto, Ontario M4N3M5, Canada

[‖]Terrence Donnelly Center for Cellular and Biomolecular Research, and Banting and Best Department of Medical Research, Department of Molecular Genetics, University of Toronto, Toronto, Ontario M5S 3E1, Canada

Supporting Information

ABSTRACT: Tumor necrosis factor-alpha (TNFα) is a pivotal component of the cytokine network linked to inflammatory diseases. Protein-based, TNFα inhibitors have proven to be clinically valuable. Here, we report the identification of short, single-stranded DNA aptamers that bind specifically to human TNFα. One such 25-base long aptamer, termed VR11, was shown to inhibit TNFα signaling as measured using NF-κB luciferase reporter assays. This aptamer bound specifically to TNFα with a dissociation constant of 7.0 ± 2.1 nM as measured by surface plasmon resonance (SPR) and showed no binding to TNFβ. Aptamer VR11 was also able to prevent TNFα-induced apoptosis as well as reduce nitric oxide (NO) production in cultured cells for up to 24 h. As well, VR11, which contains a GC rich region, did not raise an immune response when injected intraperitoneally into C57BL/6 mice when compared to a CpG oligodeoxynucleotide (ODN) control, a known TLR9 ligand. These studies suggest that VR11 may represent a simpler, synthetic scaffold than antibodies or protein domains upon which to derive nonimmunogenic oligonucleotide-based inhibitors of TNFα.

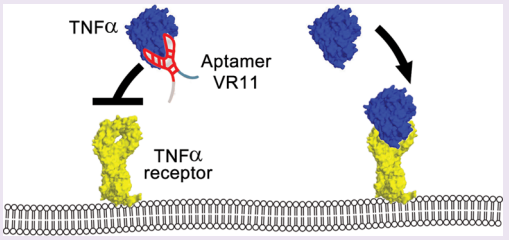

Unregulated immune responses are intimately associated with degenerative diseases such as atherosclerosis, arthritis, encephalitis, and tumors.[1−3] The primary pro-inflammatory cytokine, tumor necrosis factor alpha (TNFα), plays a critical regulatory role in enhancing these responses.[4] In the past decade, disease-modifying antirheumatic drugs (DMARDs) that target underlying immune responses processes have improved disease outcomes in patients with chronic immune response disorders.[5] Anti-TNFα protein-based therapies (Enbrel, Humira, InfliximAb) have emerged as a dominant category of DMARDs.[6] However, ∼40% of patients still display moderate to high levels of disease even after treatment with protein therapeutics, suggesting a substantial need for improved therapies.[7]

TNFα is a pro-inflammatory cytokine that is produced by an array of cell types such as macrophages, monocytes, lymphocytes, keratinocytes, and fibroblasts in response to inflammation, infection, injury, and other environmental challenges.[8] TNFα is a type 2 transmembrane protein with an intracellular amino terminus and is synthesized as a 26-kD membrane-bound protein (pro-TNFα) that is cleaved to release a soluble 17-kD TNFα molecule. TNFα has the ability to signal as a membrane-bound protein as well as a soluble cytokine. As a soluble cytokine, TNFα is active only as a noncovalently associated homotrimer.[9,10] Sufficient levels of TNFα as well as other mediators are critical for sustaining normal immune responses. TNFα can initiate host defense mechanisms to local injury but can also cause acute and chronic tissue damage.[11,12]

Despite advances in antibody and protein engineering, the major drawbacks of protein-based TNFα inhibitors are their immunogenicity arising from their chronic use and their production costs resulting in expensive therapies for patients. Simpler, synthetic, nonimmunogenic classes of TNFα inhibitors could be derived from short, single-stranded nucleic acid oligomers (ssDNA or RNA) known as aptamers. These molecules adopt a specific tertiary structure allowing them to bind to molecular targets with high specificity and affinities comparable to those of monoclonal antibodies.[13] In some cases, aptamers will display functional properties beyond just binding to their target. For instance, an aptamer to the inflammation factor human neutrophil elastase (hNE) was shown to significantly reduce lung inflammation in rats and displayed greater specificity for their target than an antielastase IgG control.[14] Examples of other aptamers exhibiting functional attributes include a DNA aptamer to anti-HIV reverse transcriptase and RNA aptamers to the basic fibroblast growth

Received: March 15, 2012
Accepted: October 9, 2012
Published: October 9, 2012

factor and vascular endothelial growth factor.[15−17] Finally, a single-stranded DNA aptamer selected to bind to thrombin has been shown to inhibit thrombin-catalyzed fibrin-clot formation *in vitro* using either purified fibrinogen or human plasma.[18]

In the present study, we constructed a 25-nucleotide variable region DNA library to perform systematic evolution of ligands by exponential enrichment (SELEX)[19] selections using recombinant TNFα as our target. Several ssDNA aptamers shown to specifically bind to TNFα were further evaluated for their ability to inhibit TNFα signaling in several independent *in vitro* assays. These analyses led to the identification of VR11, a DNA aptamer capable of inhibiting TNFα functions *in vitro*.

RESULTS AND DISCUSSION

Identification of DNA Aptamers Directed at TNFα. Traditional treatments for chronic inflammation include NSAIDs, glucocorticoids, cytostatic drugs and DMARDs. Due to the increased understanding of the molecular pathology of several inflammatory disorders, immunosuppressants, such as those directed at TNFα, have moved to the forefront of anti-inflammatory drugs. The current anti-TNFα therapy market is dominated by protein therapeutics, namely, etanercept (Enbrel), adalimumAb (Humira), and infliximAb (Remicade). These TNFα inhibitors have been shown to be therapeutically non-equivalent in terms of their structure, binding to TNFα, and their therapeutic effects.[20] More importantly, these protein-based therapeutics are large macromolecules that are costly to produce and immunogenic when used in a chronic therapy setting, with close to 40% of patients still showing disease symptoms even after treatment.

Using TNFα as a target, we perform SELEX searches with a view to identify short, synthetic DNA aptamers able to recognize this key cytokine and potentially mimic the inhibitory action of an anti-TNFα antibody (Figure 1). After 12 rounds of selection, 60 clones were sequenced and found to be enriched for 3 specific variable region (VR) sequences. Specifically, the 25-base long sequences VR1, VR2, and VR6 accounted for 20%, 13%, and 10% of the observed sequences, respectively (Table 1). Aptamers VR11 and VR20 represented unique sequences identified in this search that also selectively bound to TNFα. Aptamer VR11 was the only aptamer that inhibited human TNFα functions on cells. Interestingly, VR11 incorporates the sequence 5′-CAGTCGGCGA-3′, which was identical to a region of aptamer VR12 with the exception of a single G base insertion [5′-CAG**G**TCGGCGA-3′]. This 10-base-long conserved span represents a 40% coverage of the variable region element of our library, and despite the homology between these two sequences, VR12 displayed no inhibitory activity. This finding suggests that even a single base insertion can eliminate the functional properties of such aptamers.

In order to identify and confirm that observed sequences were specifically binding to TNFα, 96-well ELISA microtiter plates were coated with human TNFα and subsequently exposed to synthetic full-length (FL; a sequence that includes a specific VR sequence as well as the two flanking primer regions) and variable region (VR) only DNA aptamers harboring a 5′ biotin group. Aptamer binding to TNFα was confirmed with streptavidin-HRP for 20 unique sequences tested (Figure 1A) with most of them showing an ELISA signal at least double that of the control aptamers (cApt(VR), cApt(FL)).

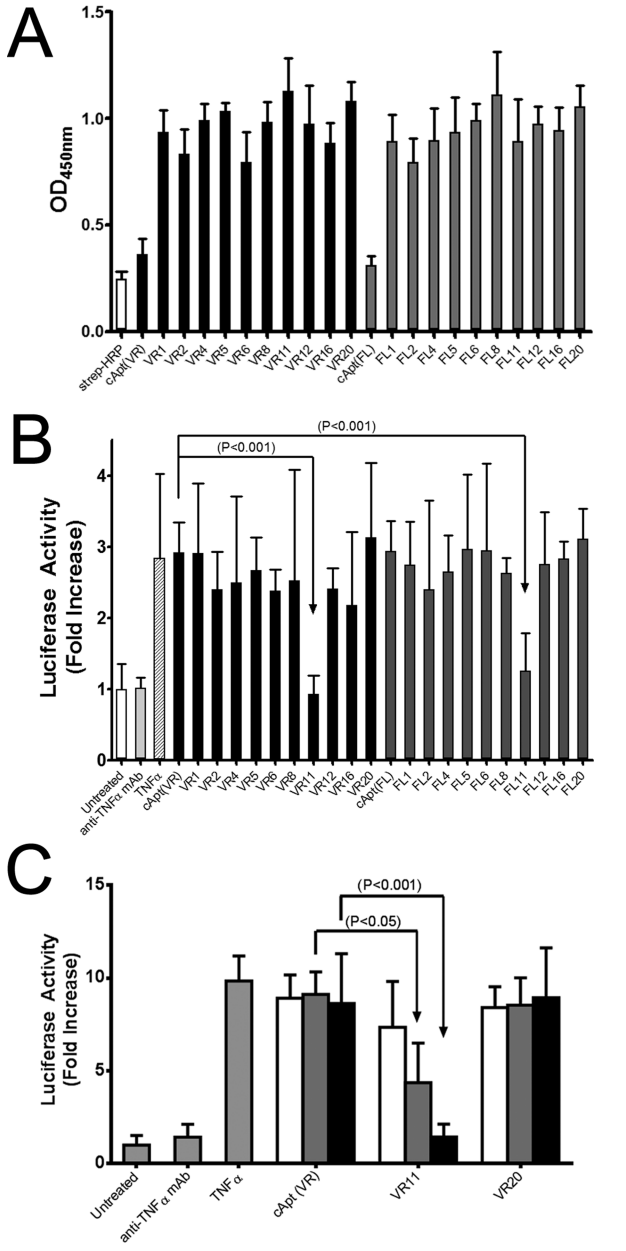

Figure 1. Binding of selected full-length (FL) and variable region (VR) DNA aptamers to TNFα and N$f\kappa$B assays identify FL11 and VR11 as TNFα inhibitors. (A) Histogram of ELISA signals confirming the binding of biotinylated FL (gray bars) and VR aptamers (black bars) to immobilized recombinant TNFα. The control DNA aptamers cApt(VR) and cApt (FL) gave ELISA signals comparable to those of wells treated with streptavidin-HRP alone (open bar). (B) Histogram of fold increase in luciferase activity in PANC-1 cells transiently transfected with a DNA plasmid construct expressing the luciferase gene under the control of N$f\kappa$B DNA binding promoter. Cells were treated with TNFα (100 ng/mL), FL (dark gray bars) and VR aptamers (black bars) or an inhibitory anti-TNFα mAb (light gray bar). Only aptamer VR11 and its full-length variant FL11 displayed inhibitory activities comparable to that of a control anti-TNFα mAb. (C) Histogram of TNFα-induced NF-κB luciferase activity in HEK293T cells. Cells were treated with 2 μM (black bars), 200 nM (gray bars), and 20 nM (white bars) of the control aptamer cApt (VR), the TNFα specific DNA aptamers VR11, VR20, as well as 20 μg/mL of the inhibitory anti-TNFα mAb. Each histogram bar represents the average enhancement in observed luciferase activity + SEM (n = 9) normalized to that of untreated samples.

dx.doi.org/10.1021/cb3003557 | *ACS Chem. Biol.* 2013, 8, 170−178

Table 1. TNFα Specific DNA Aptamer Sequences Identified from the SELEX Search As Well As Control Aptamer [cApt(VR) and cApt(FL)] Sequences Used in the Present Study

aptamer	sequence
VR1	ACAACCGACAAATTATCGCACTTAC
VR2	ATCACAGCGGGTACGAATGGCAGTG
VR4	ACGCTACGGGACTCTCAAACCGCC
VR5	AAGAACTGGCAGGCCGACCACCGGT
VR6	CGTCCGCTTTGAGTCTCGAAAAGGG
VR8	ATACCCATGGTACGACGGGCCATTC
VR11	TGGTGGATGGCGCAGTCGGCGACAA
VR12	CTCGTCAGTTCAGGTCGGCGATCAT
VR16	AGTGAGCGCTTAGTCTGCGCACTGG
VR20	TCCTCATATAGAGTGCGGGGCGTGT
cApt(VR)	AGTCAGTCAGTCAGTCAGTCAGTCA
FL1	AATTAACCCTCACTAAAGGGACAACCGACAAATTATCGCACTTACCTATAGTGTCACCTAAATCGTA
FL2	AATTAACCCTCACTAAAGGGATCACAGCGGGTACGAATGGCAGTGCTATAGTGTCACCTAAATCGTA
FL4	AATTAACCCTCACTAAAGGGACGCTACGGGACTCTCAAACCGCCCTATAGTGTCACCTAAATCGTA
FL5	AATTAACCCTCACTAAAGGGAAGAACTGGCAGGCCGACCACCGGTCTATAGTGTCACCTAAATCGTA
FL6	AATTAACCCTCACTAAAGGGCGTCCGCTTTGAGTCTCGAAAAGGGCTATAGTGTCACCTAAATCGTA
FL8	AATTAACCCTCACTAAAGGGATACCCATGGTACGACGGGCCATTCCTATAGTGTCACCTAAATCGTA
FL11	AATTAACCCTCACTAAAGGGTGGTGGATGGCGCAGTCGGCGACAACTATAGTGTCACCTAAATCGTA
FL12	AATTAACCCTCACTAAAGGGCTCGTCAGTTCAGGTCGGCGATCATCTATAGTGTCACCTAAATCGTA
FL16	AATTAACCCTCACTAAAGGGAGTGAGCGCTTAGTCTGCGCACTGGCTATAGTGTCACCTAAATCGTA
FL20	AATTAACCCTCACTAAAGGGTCCTCATATAGAGTGCGGGGCGTGTCTATAGTGTCACCTAAATCGTA
cApt(FL)	AATTAACCCTCACTAAAGGGAGTCAGTCAGTCAGTCAGTCAGTCACTATAGTGTCACCTAAATCGTA

DNA Aptamer VR11 Inhibits the Binding of TNFα to Its Receptor. NF-κB (nuclear factor kappa-light-chain enhancer of activated B cells) is a downstream eukaryotic transcription factor that is activated by various intra- and extracellular cytokines, including TNFα.[21] We selected a cell-based assay using an NF-κB luciferase reporter assay in order to define aptamer sequences that inhibited human TNFα from binding to its receptor, leading to the loss of a cell signaling event. Our preliminary screen was conducted using the human pancreatic cancer cell line PANC-1 transiently transfected with the NF-κB luciferase reporter.[22] The luciferase activity was measured 6 h post-transfection with only two DNA aptamers, namely, VR11 and FL11, displaying an ability to inhibit TNFα-dependent NF-κB expression (Figure 1B). We subsequently used a more sensitive TNFα-mediated NF-κB assay employing HEK293T cells [higher transfection efficiency] and confirmed the inhibitory ability of VR11 in a dose-dependent manner (Figure 1C). The inhibition of TNFα-mediated NF-κB signal was observed down to a VR11 aptamer concentration of 200 nM, which represented a 35-fold molar excess of aptamer over TNFα. As expected, control aptamers VR20 and cApt(VR) did not show any inhibition of TNFα-mediated signaling, suggesting that the inhibitory effects of VR11 were not due to a concentration-dependent, nonspecific binding event.

The L929 mouse fibroblast cell line was subsequently employed to define the ability of aptamer VR11 to inhibit human TNFα-induced cytotoxicity.[23] The TNFα CD_{50} value for L929 mouse fibroblast cells is approximately 3 nM (Figure 2). When L929 mouse fibroblast cells were treated with human TNFα in the presence of aptamer VR11 or an inhibitory TNFα mAb, the observed CD_{50} values were shifted to approximately 100 nM and 260 nM, respectively, representing a 33-fold and 86-fold decrease in toxicity (Figure 2). These CD_{50} values for aptamer VR11 and TNFα mAb correspond to approximately a 24-fold and 5-fold molar excess over TNFα, respectively. The control aptamer cApt(VR) as well as the TNFα-specific DNA aptamer VR20 showed no effect on the toxicity of TNFα (Figure 2). Besides the removal of the 3′ terminal A base of VR11, the truncation of bases from either the 3′ or 5′ ends of VR11 resulted in the loss of its inhibitory activity toward human TNFα (Supplementary Figure 1).

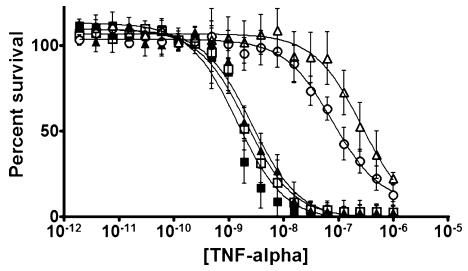

Figure 2. Aptamer VR11 inhibits TNFα-induced cytotoxicity in murine fibroblasts. L929 cells were treated with increasing concentrations of TNFα alone (▲) or in the presence of either the inhibitory anti-TNFα mAb (△), inhibitory aptamer VR11 (○), the control aptamer cApt (VR) (□), or aptamer VR20 (■). Each point represents the average % survival value ± SEM (n = 12).

The binding properties of two TNFα-binding DNA aptamers, namely, VR11 and VR20, were further characterized by surface plasmon resonance (SPR) with their binding constants determined to be in the low nanomolar range (respective K_d values of 7.0 ± 2.1 nM and 8.7 ± 2.9 nM). To assess the specificity of VR11 and VR20 for human TNFα, we also used human TNFβ as an analyte. TNFβ was chosen since it binds to TNF receptors and is the closest known homologue to TNFα having highly similar structures (Figure 3B) despite having low sequence homology (Figure 3A). It was subsequently observed that aptamers VR11 and VR20 showed no binding to TNFβ by SPR (Figure 3E and F). One feature of aptamer VR11 that may contribute to its inhibitory function may be its slow on- and off-rates (Figure 3). Once bound to TNFα, VR11 was able to block TNFα-enhanced NO

dx.doi.org/10.1021/cb3003557 | ACS Chem. Biol. 2013, 8, 170−178

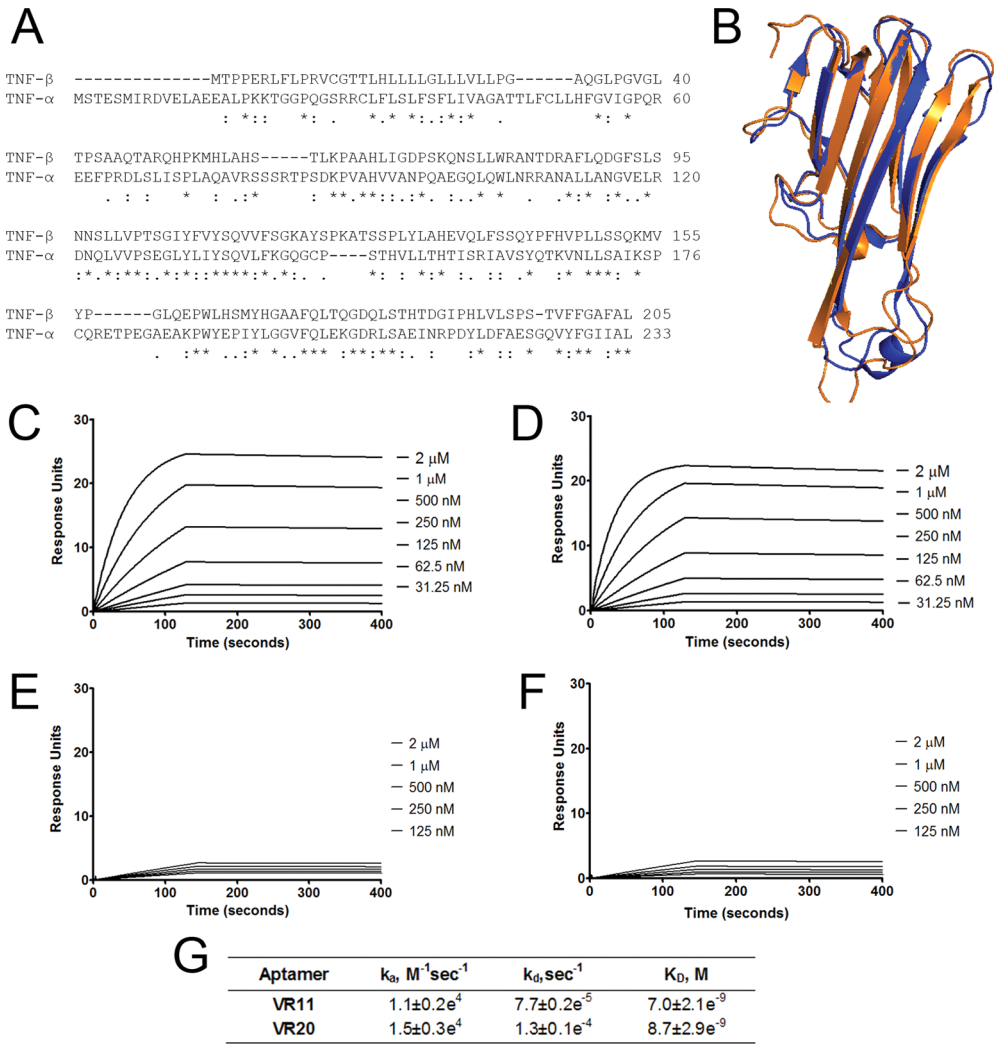

Aptamer	k_a, $M^{-1}sec^{-1}$	k_d, sec^{-1}	K_D, M
VR11	$1.1\pm0.2e^{4}$	$7.7\pm0.2e^{-5}$	$7.0\pm2.1e^{-9}$
VR20	$1.5\pm0.3e^{4}$	$1.3\pm0.1e^{-4}$	$8.7\pm2.9e^{-9}$

Figure 3. Binding kinetics of TNFα to aptamers VR11 and VR20 as determined by surface plasmon resonance. (A) Sequence alignment of soluble TNFα and the closest known homologue TNFβ. (B) Alignment of ribbon diagrams derived from the crystal structures of monomeric TNFα (orange, PBD: 1TNF) and TNFβ (blue, PDB: 1TNR). Fitted binding curves of immobilized inhibitory aptamer VR11 associated with increasing concentrations of (C) TNFα and (E) TNFβ (n = 3). Binding curves of immobilized aptamer VR20 associated with increasing concentrations of (D) TNFα and (F) TNFβ (n = 3). (G) Calculated dissociation constants (K_D) for TNFα binding to aptamer VR11 and VR20.

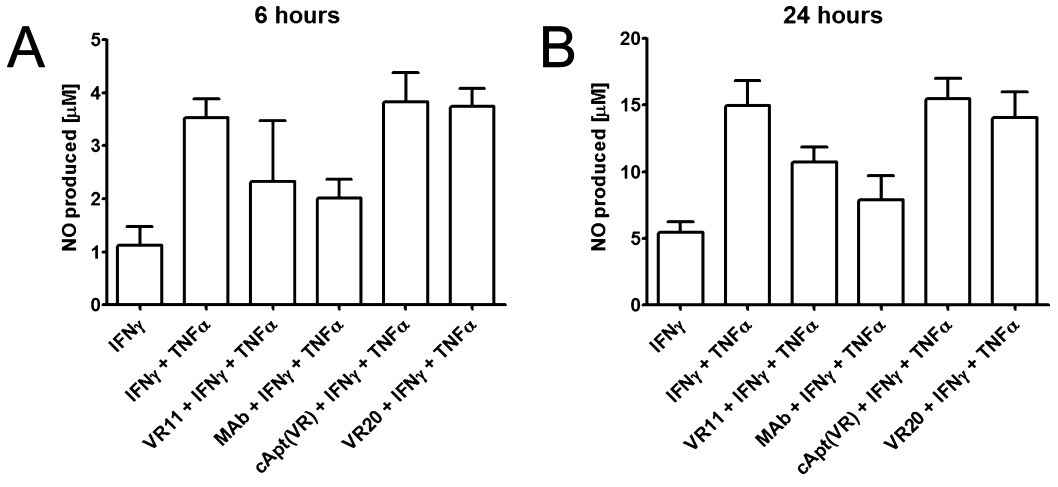

Figure 4. Inhibition of TNFα-induced NO_2^- production in macrophages. RAW264.7 cells were stimulated for (A) 6 h or (B) 24 h with IFNγ, IFNγ and TNFα or IFNγ, TNFα in the presence of either the inhibitory anti-TNFα mAb, inhibitory aptamer VR11, control aptamer cApt(VR), and aptamer VR20. The concentration of NO_2^- produced in culture medium was determined using the Griess assay. Each point represents the average amount of NO_2^- produced ± SEM (n = 9).

dx.doi.org/10.1021/cb3003557 | ACS Chem. Biol. 2013, 8, 170−178

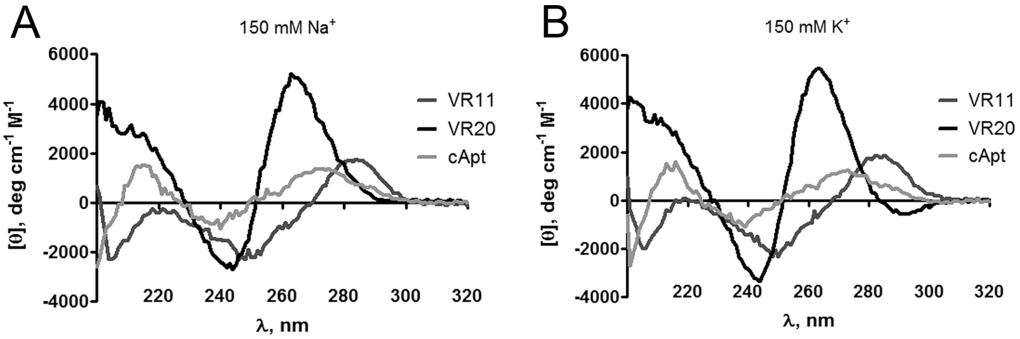

Figure 5. Structural analysis of aptamers VR11 and VR20 by circular dichroism. CD spectra of the 25-bp aptamers VR11, VR20, and cApt in the presence of either (A) sodium or (B) potassium ions.

production in macrophages over a period of 24 h (Figure 4B; as referred to as NO_2^- levels). Specifically, one of the consequences of unregulated overproduction of TNFα is the persistence of inflammation. Nitric oxide (NO) is a key mediator of inflammation stimulated by TNFα that is released by macrophages (Figure 4). We thus used the measurement of nitrite ions [NO_2^-] in solution as a marker of TNFα-induced inflammatory signaling in the macrophage cell line RAW264.7. Human TNFα alone does not elicit the release of nitrite ions from macrophages. However, a synergistic effect occurs when macrophages are concomitantly treated with interferon-gamma (IFN-γ) and TNFα.[24] At the 12 and 24 h time periods, aptamer VR11 was able to inhibit ~54% and ~45% of the TNFα-dependent NO release signal, respectively (Figure 4). In comparison, the TNFα mAb blocked ~79% and ~74% of the NO release signal over the same two time periods (Figure 4). No inhibition of TNFα-induced NO release by RAW264.7 cells was observed when treated with control aptamers cApt(VR) and VR20. This sequence thus represents a template that may be useful for modifications that may yield a suitable product for use *in vivo*.

Structural Features of DNA Aptamer VR11. The site targeted by VR11 on TNFα was not defined in the present study. The epitope recognized by the mAb to TNFα has not been identified to date, and as such this probe could not be used to locate the VR11 binding site on TNFα. In addition, the size and high avidity of this anti-TNFα mAb was able to block the binding of VR4, VR11, and VR20 TNFα-directed aptamers to their target (see Supplementary Figure 2). A structural feature of aptamer VR11 that may contribute to its inhibitory activity is its predicted G-quadruplex structure as determined by the QGRS Mapper software.[25] G-quadruplexes arise from the association of four G-bases into a cyclic Hoogsteen H-bonding arrangement. Identifying G-quadruplex structures within aptamers has been the focus of recent interest in view of the therapeutic efficacy of previously identified G-quadruplex forming ssDNA and RNA.[26−28] A case in point is the 15-mer DNA thrombin aptamer, which folds into a G-quadruplex structure.[29] Structurally, VR11 incorporates 11 guanine bases, which accounts for 44% of its sequence. G-quadruplexes typically occur when 3 or more consecutive G bases are present within a sequence.[30] However, the G-rich content of VR11 sequence displays an 18-base-long stretch containing 4 GG repeats (5′-**GG**T**GG**AT**GG**CGCAGTC**GG**-3′) that may stabilize the aptamer.[31] Interestingly, the DNA aptamer KS-B, specific for thrombin, also incorporates 4 GG repeats within its sequence (GGTTGGTGTGGTTGG) and adopts an intramolecular G-quadruplex structure (monomeric chair form) as proven from its crystal structure.[32−34] Thus, the projected G-quadruplex for VR11 may exist in solution. An intramolecular G-quartet structure[35,36] within VR11 would support our SPR data that suggest a 1:1 association of VR11 with TNFα. The circular dichroism spectra of VR11, VR20, and the control aptamer cApt were thus recorded in order to monitor for the possible occurrence of a G-quadruplex structure within these DNA aptamers. The sequence of VR20 harbors 4 consecutive G bases [Table 1; 5′-CGGGGC-3′motif], and its CD spectrum displays a negative ellipticity band centered around 240 nm as well as a positive band near 260 nm. This spectrum indicates that the GGGG motif present within VR20 adopts a characteristic G-quadruplex structure in solution with a stacking pattern involving guanosines having identical glycosidic bond angles giving rise to a four-stranded parallel quadruplex structure typically observed for the motif 5′-TGGGGT-3′.[37,38] The CD spectrum of control aptamer cApt did not reveal any known spectral features indicative of G-quadruplexes. As for VR11, its CD spectrum harbors a broad positive band around 290 nm, suggesting that guanosines with different glycosidic bond angles within its sequence are stacked in the presence of sodium or potassium (Figure 5A and B). Unlike the CD spectrum observed for VR20, the VR11 spectrum does not provide conclusive proof that the guanosine elements within its 25-bp sequence are arranged in a traditional G-quadruplex structure. Nevertheless, a structural arrangement involving the stalking of guanosine bases is present in VR11 and may stabilize its structure. Aptamer stability is crucial for targeting TNFα since the effectiveness of current protein-based therapies can be partly attributed to their long circulating half-lives, such as Etanercept, which is linked to the Fc portion of an IgG1 to help extend its half-life to 4−5 days, or the PEGylation of anti-TNF antibodies.[39,40] Recently, some of the most common modifications of aptamers investigated have been their conjugation to poly(ethylene glycol) (PEG) groups for increased stability.[41,42] In addition, to increase the *in vivo* circulating half-life of DNA aptamers, modified nucleotides could be introduced into the libraries during synthesis such as 2′-OH group with 2′-fluoro or 2′-amino, aromatic, or alkyl moieties or introduction of locked nucleic acid (LNA).[43,44] Also, aptamer libraries with longer variable regions may identify sequences with a higher G-rich content, which in turn could adopt different G-quadruplex structures and yield improved inhibitors to TNFα.[45]

Immunogenicity of DNA Aptamer VR11. One therapeutic obstacle that DNA aptamers may encounter is their possible activation of an immune response similar to that of oligodeoxynucleotides containing CpG motifs. These CpG

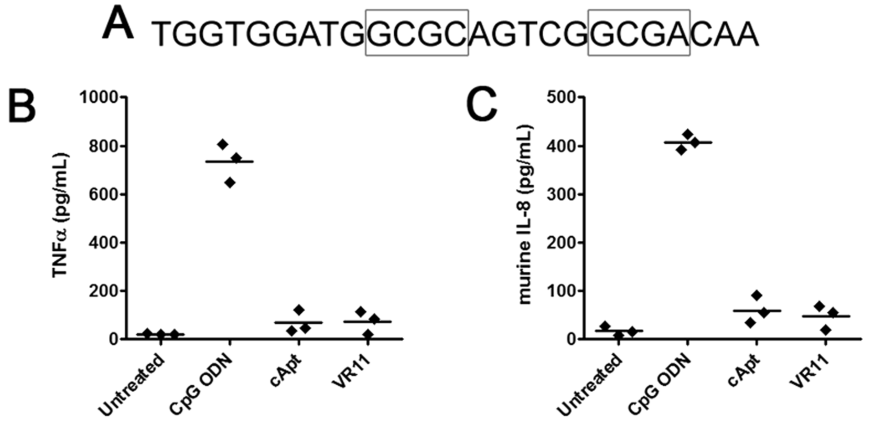

Figure 6. Aptamer VR11 does not cause an innate immune response *in vivo*. (A) Potential CpG motifs located in the variable region of aptamer VR11. C57BL/6 mice (n = 3) were given an intraperitoneal injection of 10 μg of CpG ODN, 100 μg of aptamer VR11 or cApt, and the amount of (B) TNFα or (C) mIL-8 in serum 3 h after injection was determined by ELISA.

motifs can promote a Th1 response by signaling through TLR9, which is expressed on human B cells and plasmacytoid dendritic cells leading to an innate immune response.[46,47] VR11 contains two possible CpG motif sequences (Figure 6A). To test whether this DNA aptamer can induce an innate immune response, we injected 100 μg of aptamer VR11 and cApt as well as 10 μg of a known TLR9 ligand CpG ODN in the intraperitoneal cavity of C57BL/6 mice and quantified the amount of TNFα and mouse IL-8 present in their serum after 3 h. The CpG ODN positive control yielded a 35-fold increase in TNFα and a 24-fold increase in murine IL-8 serum levels, while the control aptamer cApt (which contains no CpG motifs) and the TNFα-specific VR11 DNA aptamer yielded statistically nonsignificant increases in both TNFα and murine IL-8 cytokine levels as compared to untreated mice (Figure 6B and C).

Summary. Short DNA oligonucleotides such as aptamers are considered to be nonimmunogenic. This study also establishes that VR11 does not trigger an innate immune response associated with the production of inflammatory cytokines (Figure 6), which is relevant since TNFα antagonists are now well established as an effective treatment for an array of inflammatory disorders in which TNFα plays an important pathological role. Current protein-based therapies have been effective, although these agents have now been shown to display immunogenicity following their long-term use. As well, a significant proportion of patients with inflammatory disorders are nonresponders to such protein-based therapeutics.[48] Although DNA-based aptamers are small, synthetic targeting agents, they still face several obstacles to overcome as therapeutic agents. Aptamer VR11 does provide a simple scaffold for developing DNA-based inhibitors of TNFα with pharmacological properties distinct from those of existing classes of therapeutic agents aimed at treating inflammatory diseases.

METHODS

Expression and Purification of Human TNFα. The expression plasmid (RCA-093) encoding a soluble 157-amino acid long, His-tagged human TNFα recombinant protein (residues 77−233) was obtained from Bioclone Inc. The protein was expressed in *Escherichia coli* BL21 (DE3) strain. The expression of the TNFα (77−233) fragment was induced in culture overnight with isopropyl β-D-thiogalactopyranoside (IPTG, 0.5 mM). Soluble human TNFα was purified by nickel affinity chromatography under nondenaturing conditions. Purified human TNFα was characterized by SDS-PAGE and quantified using the Bradford assay.[49] To verify that the protein was properly folded and functionally active, a cytotoxicity assay was performed using the L929 cell line sensitized with actinomycin D and compared to a commercial recombinant human TNFα purchased from Bioclone Inc. (Supplementary Figure 3).

Aptamer Identification. The initial ssDNA library contained a central randomized sequence of 25 nucleotides flanked by T3 and SP6 primer regions, respectively. Briefly, the sequence of the starting library was 5′ AAT TAA CCC TCA CTA AAG GG-(25N)-CTA TAG TGT CAC CTA AAT CGTA. The forward primer 5′ AAT TAA CCC TCA CTA AAG GG 3′ and reverse primer 5′ TAC GAT TTA GGT GAC ACT ATA G 3′ were used for selection and cloning (IDT Technologies, Inc.). To begin the selection, a 50 nmol aliquot of the library representing ~3.0 × 10^{16} molecules consisting of ~25 copies of each possible unique sequence was first counter-selected against a 6-His peptide (HHHHHH) loaded onto Ni-NTA magnetic agarose beads. The resulting sub-library was then exposed to 10 μg of His-tagged TNFα immobilized onto Ni-NTA beads suspended in Selection Buffer (PBS, 0.005% (v/v) Tween-20) at 37 °C for 1 h. Unbound DNA sequences were washed away (PBS, 0.005% (v/v) Tween-20), and DNA−protein complexes were eluted from the recovered beads using an imidazole buffer (PBS, 0.005% (v/v) Tween-20, 240 mM imidazole). The ssDNA component was precipitated with sodium perchlorate/isopropanol and recaptured using a silica membrane-based purification system (Qiagen Inc.). The DNA aptamers were then amplified by asymmetrical PCR using a 100-fold excess of forward primer. After every three subsequent rounds of selection, the amount of target was reduced in half to increase the selection pressure to capture the tightest binding species. After 12 rounds of selection, the bound sequences were amplified by PCR, cloned into a pCR4-TOPO TA vector (Invitrogen), and analyzed using BioEdit sequence alignment editor software (Ibis Therapeutics).

Aptamer-Based Enzyme Linked Binding Assay. A 96-well ELISA microtiter plate (BD Falcon) was coated overnight at 4 °C with 100 μL of human TNFα (10 μg/mL) prepared in coating buffer (0.2 M carbonate/bicarbonate, pH 9.4). The plate was then washed 3 times with PBS-T (0.1 M phosphate, 0.15 M sodium chloride, pH 7.0 containing 0.05% Tween-20) and blocked overnight at 4 °C in 150 μL of blocking solution (PBS-T + 1% (w/v) BSA). The plate was washed 3 times with PBS-T and incubated overnight at 4 °C with 100 μL (10 μg/mL) of 5′ biotinylated aptamers dissolved in PBS, 0.005% (v/v) Tween-20. The plates were washed and incubated for 1 h at 4 °C with 100 μL of streptavidin-HRP (1:2000). Plates were then read on a plate reader at 450 nm following washing and dispensing of 100 μL of TMB substrate (1 TMB tablet (Sigma-Aldrich Inc.) dissolved in 1 mL of DMSO in 10 mL of 0.05 M phosphate citrate, pH 5.0 and 2 μL sodium peroxide) per well. Color development was stopped by adding 50 μL of 1 M sulphuric acid per well.

dx.doi.org/10.1021/cb3003557 | ACS Chem. Biol. 2013, 8, 170−178

NF-κB Luciferase Reporter Assay. An NF-κB luciferase reporter plasmid was transfected into cells as a marker of TNFα binding as previously described.[22] Briefly, 0.1 μg/well TA-LUC NF-κB and 10 ng/well β-gal CMV were co-transfected into the cells. PANC1 (ATCC) (1.0×10^4) and HEK293T (ATCC) (5.0×10^3) cells were seeded in a 96-well plate 24 h before the transfection steps. DNA was transfected into cells using Lipofectamine 2000 (Invitrogen Canada Inc.). Cells were incubated 4−6 h in Opti-mem medium (Promega) and transferred to 10% FBS DMEM overnight. Aptamers were added to the medium (1 μM final concentration for PANC-1 cells or 2 μM, 200 nM, and 20nM for HEK293T) 30 min prior to treating the transfected cells with recombinantly expressed human TNFα (100 ng/mL). Luciferase activity was measured after 6 h using the Dual-Light System luciferase assay from Applied Biosystems according to the manufacturer's protocol and read on a Luminoskan Ascent luminometer (ThermoLab Systems). The results were normalized to the values obtained for β-galactosidase activity.

Inhibition of TNFα-Induced Cytotoxicity. L929 cells (ATCC) were seeded 24 h before experiments in 96-well flat-bottom microtiter plates at a density of 1.0×10^4 cells/well in DMEM medium containing 10% FBS. Aptamers (2 μM) or 20 μg/mL anti-TNFα mAb (R&D systems) were incubated with human TNFα for 2 h in PBS prior to incubation with cells. Subsequently, aptamer-TNFα samples were added to the cells for 2 h. Cells were then washed with warm PBS and incubated in complete medium for another 48 h. The viability of adherent cells was subsequently determined using the sulforhodamine B assay.[50]

Surface Plasmon Resonance. All experiments were performed using the ProteOn XPR36 protein interaction array system (Bio-Rad Laboratories, Inc.) and one ProteOn NLC sensor chip, coated with NeutrAvidin for coupling of biotinylated molecules. Biotinylated aptamers VR11, VR20, and rApt(VR) were synthesized with a 5′ biotin with a standard C6 spacer and HPLC purified (Integrated DNA Technologies, Inc.). Subsequently 2.5 nM of aptamer was diluted in PBS-T and injected for 30 s at 30 μL/min. Aptamer loading on the chip yielded approximately 10−12 response units, which represented ∼1 ng of aptamer. Human TNFα and TNFβ stock solutions were diluted as a series of 2-fold dilutions ranging from 2 μM to 3.9 nM in PBS-T (0.05% (v/v) Tween-20) pH 7.4 (Figure 3C−F). Protein concentrations and a buffer control were injected in the analyte channel with a contact time of 120 s, dissociation time of 800 s, and a flow rate of 100 μL/min. The ligand channels were regenerated with a 30 s injection of 1 M H_3PO_4 followed by a 30 s injection of 1 M NaCl. All experiments were performed at 25 °C and repeated in triplicate. Sensorgrams were then double-referenced by subtracting the buffer response and using the interspot reference. The sensorgrams were fitted globally to a 1:1 Langmuir binding model, and the kinetic parameters for the association (k_a), dissociation rates (k_d), and binding constant (K_D) were derived from the fitted curves.

Determination of Aptamer Concentration and Circular Dichroism Spectroscopy. The oligonucleotide concentration of each aptamer solution was determined from its absorbance at 260 nm as measured at 25 °C with a Cary 300 Bio spectrophotometer (Varian Canada, Inc.) using molar extinction coefficients of 244 400 M^{-1} cm^{-1}, 239 400 M^{-1} cm^{-1}, and 251 800 M^{-1} cm^{-1} for VR11, VR20, and cApt respectively. Circular dichroism (CD) spectra were recorded at 25 °C using an Aviv model 62 DS spectropolarimeter (Aviv Associates). The buffer used for CD measurements contained 10 mM phosphate, 0.1 mM EDTA (free acid), and 100 mM of either sodium or potassium ions. Either KOH or NaOH was added to the buffers until pH 7 was reached, and the ionic strengths of the buffers were adjusted to the desired level by adding known amounts of NaCl or KCl. Dry and desalted DNA aptamers were dissolved in the buffers until a concentration of ∼0.03 mM was achieved. The DNA aptamer solutions were heated to 100 °C for 5 min to transform the DNA aptamer into their unfolded forms and slowly allowed to cool to 25 °C. Ellipticity values (reported as θ) were measured from 320 to 200 nm in 1 nm increments using a quartz cuvette with an optical path length of 0.1 cm.

Inhibition of TNFα-Induced NO Production in Macrophages. Experiments were modified using a previous protocol.[51] Briefly, RAW 264.7 cells (ATCC) were seeded at a density of 1.0×10^5 cells/well in a 12-well plate in RPMI 1640 + 10% FBS. Cells were pretreated for 1 h with 2 U/mL IFN-γ (Peprotech) and then treated with 100 ng/mL of human TNFα in 1 mL of medium with aptamers VR11, VR20, or the control aptamer cApt(VR) at a final concentration of 2 μM or with 10 μg/mL anti-TNF mAb. Aliquots of the medium [100 μL] were removed at each time point, and the NO_2^- level was determined using the Griess reagent kit for nitrite determination (Invitrogen).

Analysis of VR11 Ability To Activate an Innate Immune Response. The aptamer VR11 and cApt were dissolved in sterilized saline at a concentration of 500 μg/mL, and CpG ODN (5′-TCCATGACGTTCCTGACGTT-3′; type B murine, ODN 1826, Invivogen) was dissolved at a concentration of 50 μg/mL. Intraperitoneal injections (200 μL) were administered in C57BL/6 mice. The untreated group received an injection of 200 μL of saline alone. Three hours after injection, mice were sacrificed, and their serum was collected for analysis. Protein cytokine concentrations were determined using the DuoSet ELISA development kits for mouse CXCL1/KC (murine IL-8, R & D systems Inc.) and murine TNFα (R & D systems Inc.) as per manufacturers protocols. Animals were kept under standard pathogen-free conditions at the Ontario Cancer Institute animal facility. Experiments were performed in accordance with the rules and regulations of the Canadian Council for Animal Care.

■ ASSOCIATED CONTENT

Ⓢ Supporting Information

This material is available free of charge *via* the Internet at http://pubs.acs.org.

■ AUTHOR INFORMATION

Corresponding Author

*E-mail: gariepy@sri.utoronto.ca.

Notes

The authors declare no competing financial interest.

■ ACKNOWLEDGMENTS

We wish to thank S. Mamaghani and D. Hedley for providing access to TA-LUC NF-κB, β-gal CMV, and PANC1 cells. We would also like to thank T. Watts for providing the HEK293T cells and also K. Geddes and D. Philpott for help with immune monitoring assays. This work was supported by an operating grant from the Canadian Breast Cancer Foundation (J.G.) and a studentship award to E.W.O. from the Canadian Institutes of Health Research Training Program in Biological Therapeutics.

■ REFERENCES

(1) Feldmann, M., and Maini, R. N. (2001) Anti-TNF alpha therapy of rheumatoid arthritis: what have we learned? *Annu. Rev. Immunol. 19*, 163−196.

(2) Borish, L. C., and Steinke, J. W. (2003) 2. Cytokines and chemokines. *J. Allergy Clin. Immunol. 111*, S460−475.

(3) van den Berg, W. B. (2001) Anti-cytokine therapy in chronic destructive arthritis. *Arthritis Res. 3*, 18−26.

(4) Furst, D. E., Wallis, R., Broder, M., and Beenhouwer, D. O. (2006) Tumor necrosis factor antagonists: different kinetics and/or mechanisms of action may explain differences in the risk for developing granulomatous infection. *Semin. Arthritis Rheum. 36*, 159−167.

(5) Smolen, J. S., Aletaha, D., Koeller, M., Weisman, M. H., and Emery, P. (2007) New therapies for treatment of rheumatoid arthritis. *Lancet 370*, 1861−1874.

(6) Mount, C., and Featherstone, J. (2005) Rheumatoid arthritis market. *Nat. Rev. Drug Discovery 4*, 11−12.

(7) Mierau, M., Schoels, M., Gonda, G., Fuchs, J., Aletaha, D., and Smolen, J. S. (2007) Assessing remission in clinical practice. *Rheumatology (Oxford) 46*, 975−979.
(8) Carswell, E. A., Old, L. J., Kassel, R. L., Green, S., Fiore, N., and Williamson, B. (1975) An endotoxin-induced serum factor that causes necrosis of tumors. *Proc. Natl. Acad. Sci. U.S.A. 72*, 3666−3670.
(9) Locksley, R. M., Killeen, N., and Lenardo, M. J. (2001) The TNF and TNF receptor superfamilies: integrating mammalian biology. *Cell 104*, 487−501.
(10) Hehlgans, T., and Pfeffer, K. (2005) The intriguing biology of the tumour necrosis factor/tumour necrosis factor receptor superfamily: players, rules and the games. *Immunology 115*, 1−20.
(11) Beutler, B. A. (1999) The role of tumor necrosis factor in health and disease. *J. Rheumatol. Suppl. 57*, 16−21.
(12) Feldmann, M., and Maini, S. R. (2008) Role of cytokines in rheumatoid arthritis: an education in pathophysiology and therapeutics. *Immunol. Rev. 223*, 7−19.
(13) Ellington, A. D., and Szostak, J. W. (1990) In vitro selection of RNA molecules that bind specific ligands. *Nature 346*, 818−822.
(14) Bless, N. M., Smith, D., Charlton, J., Czermak, B. J., Schmal, H., Friedl, H. P., and Ward, P. A. (1997) Protective effects of an aptamer inhibitor of neutrophil elastase in lung inflammatory injury. *Curr. Biol. 7*, 877−880.
(15) Schneider, D. J., Feigon, J., Hostomsky, Z., and Gold, L. (1995) High-affinity ssDNA inhibitors of the reverse transcriptase of type 1 human immunodeficiency virus. *Biochemistry 34*, 9599−9610.
(16) Jellinek, D., Lynott, C. K., Rifkin, D. B., and Janjic, N. (1993) High-affinity RNA ligands to basic fibroblast growth factor inhibit receptor binding. *Proc. Natl. Acad. Sci. U.S.A. 90*, 11227−11231.
(17) Jellinek, D., Green, L. S., Bell, C., and Janjic, N. (1994) Inhibition of receptor binding by high-affinity RNA ligands to vascular endothelial growth factor. *Biochemistry 33*, 10450−10456.
(18) Bock, L. C., Griffin, L. C., Latham, J. A., Vermaas, E. H., and Toole, J. J. (1992) Selection of single-stranded DNA molecules that bind and inhibit human thrombin. *Nature 355*, 564−566.
(19) Tuerk, C., and Gold, L. (1990) Systematic evolution of ligands by exponential enrichment: RNA ligands to bacteriophage T4 DNA polymerase. *Science 249*, 505−510.
(20) van Vollenhoven, R. F. (2007) Switching between anti-tumour necrosis factors: trying to get a handle on a complex issue. *Ann. Rheum. Dis. 66*, 849−851.
(21) Sen, R., and Baltimore, D. (1986) Inducibility of kappa immunoglobulin enhancer-binding protein Nf-kappa B by a posttranslational mechanism. *Cell 47*, 921−928.
(22) Mamaghani, S., Patel, S., and Hedley, D. W. (2009) Glycogen synthase kinase-3 inhibition disrupts nuclear factor-kappaB activity in pancreatic cancer, but fails to sensitize to gemcitabine chemotherapy. *BMC Cancer 9*, 132.
(23) Matthews, N., Neale, M. L., Jackson, S. K., and Stark, J. M. (1987) Tumour cell killing by tumour necrosis factor: inhibition by anaerobic conditions, free-radical scavengers and inhibitors of arachidonate metabolism. *Immunology 62*, 153−155.
(24) Paludan, S. R. (2000) Synergistic action of pro-inflammatory agents: cellular and molecular aspects. *J. Leukocyte Biol. 67*, 18−25.
(25) Kikin, O., D'Antonio, L., and Bagga, P. S. (2006) QGRS Mapper: a web-based server for predicting G-quadruplexes in nucleotide sequences. *Nucleic Acids Res. 34*, W676−682.
(26) Bates, P. J., Kahlon, J. B., Thomas, S. D., Trent, J. O., and Miller, D. M. (1999) Antiproliferative activity of G-rich oligonucleotides correlates with protein binding. *J. Biol. Chem. 274*, 26369−26377.
(27) Xu, X., Hamhouyia, F., Thomas, S. D., Burke, T. J., Girvan, A. C., McGregor, W. G., Trent, J. O., Miller, D. M., and Bates, P. J. (2001) Inhibition of DNA replication and induction of S phase cell cycle arrest by G-rich oligonucleotides. *J. Biol. Chem. 276*, 43221−43230.
(28) Marchand, C., Pourquier, P., Laco, G. S., Jing, N., and Pommier, Y. (2002) Interaction of human nuclear topoisomerase I with guanosine quartet-forming and guanosine-rich single-stranded DNA and RNA oligonucleotides. *J. Biol. Chem. 277*, 8906−8911.
(29) Russo Krauss, I., Merlino, A., Giancola, C., Randazzo, A., Mazzarella, L., and Sica, F. (2011) Thrombin-aptamer recognition: a revealed ambiguity. *Nucleic Acids Res. 39*, 7858−7867.
(30) Randazzo, A., Spada, G. P., and Silva, M. W. (2012) Circular dichroism of quadruplex structures. *Top. Curr. Chem.*, DOI: 10.1007/128_2012_331.
(31) Collie, G. W., and Parkinson, G. N. (2011) The application of DNA and RNA G-quadruplexes to therapeutic medicines. *Chem. Soc. Rev. 40*, 5867−5892.
(32) Macaya, R. F., Schultze, P., Smith, F. W., Roe, J. A., and Feigon, J. (1993) Thrombin-binding DNA aptamer forms a unimolecular quadruplex structure in solution. *Proc. Natl. Acad. Sci. U.S.A. 90*, 3745−3749.
(33) Padmanabhan, K., Padmanabhan, K. P., Ferrara, J. D., Sadler, J. E., and Tulinsky, A. (1993) The structure of alpha-thrombin inhibited by a 15-mer single-stranded DNA aptamer. *J. Biol. Chem. 268*, 17651−17654.
(34) Wang, K. Y., Krawczyk, S. H., Bischofberger, N., Swaminathan, S., and Bolton, P. H. (1993) The tertiary structure of a DNA aptamer which binds to and inhibits thrombin determines activity. *Biochemistry 32*, 11285−11292.
(35) Williamson, J. R. (1994) G-quartet structures in telomeric DNA. *Annu. Rev. Biophys. Biomol. Struct. 23*, 703−730.
(36) Gilbert, D. E., and Feigon, J. (1999) Multistranded DNA structures. *Curr. Opin. Struct. Biol. 9*, 305−314.
(37) Hardin, C. C., Henderson, E., Watson, T., and Prosser, J. K. (1991) Monovalent cation induced structural transitions in telomeric DNAs: G-DNA folding intermediates. *Biochemistry 30*, 4460−4472.
(38) Hardin, C. C., Watson, T., Corregan, M., and Bailey, C. (1992) Cation-dependent transition between the quadruplex and Watson-Crick hairpin forms of d(CGCG3GCG). *Biochemistry 31*, 833−841.
(39) Mohler, K. M., Torrance, D. S., Smith, C. A., Goodwin, R. G., Stremler, K. E., Fung, V. P., Madani, H., and Widmer, M. B. (1993) Soluble tumor necrosis factor (TNF) receptors are effective therapeutic agents in lethal endotoxemia and function simultaneously as both TNF carriers and TNF antagonists. *J. Immunol. 151*, 1548−1561.
(40) Choy, E. H., Hazleman, B., Smith, M., Moss, K., Lisi, L., Scott, D. G., Patel, J., Sopwith, M., and Isenberg, D. A. (2002) Efficacy of a novel PEGylated humanized anti-TNF fragment (CDP870) in patients with rheumatoid arthritis: a phase II double-blinded, randomized, dose-escalating trial. *Rheumatology (Oxford) 41*, 1133−1137.
(41) Willis, M. C., Collins, B. D., Zhang, T., Green, L. S., Sebesta, D. P., Bell, C., Kellogg, E., Gill, S. C., Magallanez, A., Knauer, S., Bendele, R. A., Gill, P. S., and Janjic, N. (1998) Liposome-anchored vascular endothelial growth factor aptamers. *Bioconjugate Chem. 9*, 573−582.
(42) Healy, J. M., Lewis, S. D., Kurz, M., Boomer, R. M., Thompson, K. M., Wilson, C., and McCauley, T. G. (2004) Pharmacokinetics and biodistribution of novel aptamer compositions. *Pharm. Res. 21*, 2234−2246.
(43) Schoetzau, T., Langner, J., Moyroud, E., Roehl, I., Vonhoff, S., and Klussmann, S. (2003) Aminomodified nucleobases: functionalized nucleoside triphosphates applicable for SELEX. *Bioconjugate Chem. 14*, 919−926.
(44) Barciszewski, J., Medgaard, M., Koch, T., Kurreck, J., and Erdmann, V. A. (2009) Locked nucleic acid aptamers. *Methods Mol. Biol. 535*, 165−186.
(45) Burge, S., Parkinson, G. N., Hazel, P., Todd, A. K., and Neidle, S. (2006) Quadruplex DNA: sequence, topology and structure. *Nucleic Acids Res. 34*, 5402−5415.
(46) Krieg, A. M. (2002) CpG motifs in bacterial DNA and their immune effects. *Annu. Rev. Immunol. 20*, 709−760.
(47) Krug, A., Rothenfusser, S., Hornung, V., Jahrsdorfer, B., Blackwell, S., Ballas, Z. K., Endres, S., Krieg, A. M., and Hartmann, G. (2001) Identification of CpG oligonucleotide sequences with high induction of IFN-alpha/beta in plasmacytoid dendritic cells. *Eur. J. Immunol. 31*, 2154−2163.
(48) Van Assche, G. (2011) Immunogenicity of anti-TNF antibodies. Has the veil been lifted? *Gut 60*, 285−286.

(49) Bradford, M. M. (1976) A rapid and sensitive method for the quantitation of microgram quantities of protein utilizing the principle of protein-dye binding. *Anal. Biochem. 72*, 248−254.
(50) Skehan, P., Storeng, R., Scudiero, D., Monks, A., McMahon, J., Vistica, D., Warren, J. T., Bokesch, H., Kenney, S., and Boyd, M. R. (1990) New colorimetric cytotoxicity assay for anticancer-drug screening. *J. Natl. Cancer Inst. 82*, 1107−1112.
(51) Ding, A. H., Nathan, C. F., and Stuehr, D. J. (1988) Release of reactive nitrogen intermediates and reactive oxygen intermediates from mouse peritoneal macrophages. Comparison of activating cytokines and evidence for independent production. *J. Immunol. 141*, 2407−2412.